Digital Signal Processing 23 (2013) 1773–1782

Contents lists available at SciVerse ScienceDirect

Digital Signal Processing

www.elsevier.com/locate/dsp

An improved class of multiplierless decimation filters: Analysis and design ☆

G. Jovanovic Dolecek [a,*], M. Laddomada [b]

[a] Department of Electronics, Institute INAOE, Puebla, Mexico
[b] Electrical Engineering Department, Texas A&M University-Texarkana, USA

ARTICLE INFO

Article history:
Available online 6 June 2013

ABSTRACT

In this paper, we present a class of low-complexity decimation filters for oversampled discrete-time signals. The proposed class of filters improves the frequency response of classical comb filters in two respects. First, it introduces extra-attenuation around the so-called folding bands, i.e., frequency intervals whose spurious signals are folded down to baseband during the decimation process. Second, this class reduces the passband distortion via an effective droop-compensator block, thus increasing the passband of the decimation filters. Like comb filters, the proposed class can be realized through multiplierless architectures, which are also discussed thoroughly in the paper. Unlike comb filters, the proposed filters have superior spurious signal rejection and a greatly reduced droop in the signal passband. These features make the proposed filters suitable for multistage decimation applications, such as reconfigurable software radio receivers, as well as for decimating oversampled digital signals produced by $\Sigma\Delta$ A/D converters. The paper discusses several useful techniques for designing the proposed filters in a variety of architectures with emphasis on non-recursive architectures. Design examples are discussed to highlight the key frequency features along with implementation issues aimed at reducing the computational complexity of the filters.

1. Introduction

Computationally efficient multistage decimation filters are key components in wide-band, multi-standard, reconfigurable receivers [1–5]. Multistage decimation filters [6,7] are also widely used to decimate signals oversampled by $\Sigma\Delta$ Analog-to-Digital (A/D) converters [8], and for digital down-converters as employed in digital receivers [9,10].

An essential block in a multistage decimation architecture is the comb filter, which can be effectively implemented with only additions and subtractions [11]. However, the magnitude response features poor attenuation around the folding bands and a considerable passband distortion that deteriorates the sampled signal. Several works in the literature have proposed a variety of solutions to improve the frequency response of classical comb filters, including a work addressing the use of comb filters in multirate applications [12].

In [13] the authors proposed the design of decimation filters based on the first 104 cyclotomic polynomials, which was later extended in [14] over the first 200 cyclotomic polynomials. A 3rd-order modified decimation sinc filter was proposed in [15]. The class of comb filters was then generalized in [16] whereby the authors proposed an optimization framework for deriving the optimal zero rotations of Generalized Comb Filters (GCFs) for any filter order and decimation factor M. In [17] generalized comb filters are implemented in non-recursive architecture by exploiting polyphase decomposition. In [18] the authors proposed a multiplierless architecture for the design of 3rd-order GCFs. In [19], the authors proposed a novel two-stage non-recursive architecture for the design of generalized comb filters.

In [20] authors proposed computational efficient architectures for classical comb filters used for multirate applications. Comb filters were used as constituent blocks in Kaiser and Hamming [21] sharpened structures in [22], while in [23] the authors proposed several architectures for comb filters including sharpened structures. In [24] the authors addressed the design of a novel two-stage sharpened comb decimator. In [25] the authors proposed novel decimation schemes for $\Sigma\Delta$ A/D converters based on Kaiser and Hamming sharpened filters. A novel multistage comb rotated sinc filter with sharpened response was proposed in [26]. In [27] the authors proposed a new decimation filter improving the frequency response of Cascaded-Integrator-Comb (CIC) Decimation Filters, while in [28] a simple method to compensate for the passband distortion of CIC decimation filters was proposed.

☆ This work has been partially supported by the US National Science Foundation under Grant No. 0925080.

* Corresponding author.
E-mail addresses: gordana@inaoep.mx (G. Jovanovic Dolecek), mladdomada@tamut.edu (M. Laddomada).

1051-2004/$ – see front matter
http://dx.doi.org/10.1016/j.dsp.2013.05.011

A new cascaded modified CIC-cosine decimation filter was proposed in [29]. In [30] the authors addressed the synthesis of very sharp decimators and interpolators using the frequency-response masking technique. Finally, in [31] the authors recently proposed sharpening of CIC filters with a Chebyshev polynomial resulting in equi-ripple and wider controlled stopbands.

The main goal of this paper is to propose a reconfigurable, multiplierless, low-complexity decimation filter architecture that, compared to recursive implementation of comb filters, i.e., CIC architectures, features 1) improved passband magnitude response, 2) improved stopband magnitude response around the folding bands of CIC filters, 3) no integrator section operating at high input sample rate, and 4) low-power consumption. Moreover, the paper provides several hints to reduce the computational complexity of the proposed filters by exploiting polyphase decomposition. Non-recursive architectures are discussed by focusing on specific decimation filters.

The rest of the paper is organized as follows. We first introduce the z-transfer function of the proposed class of filters in Section 2, where we also highlight its key features. In this section we also discuss the design of such filters by addressing the choice of key design parameters. Section 3 presents several examples aimed at contrasting the magnitude response of the proposed filters with classical comb filters. Several effective architectures for implementing the proposed decimation filters are discussed in Section 4, while comparisons with state-of-the-art techniques are presented in Section 5. Finally, Section 6 draws the conclusion.

2. The proposed decimation filters

The objective of this section is to introduce the notation used throughout the paper along with the proposed class of decimation filters and the criteria for the choice of the key filter parameters.

2.1. Notation

Let us briefly describe the notation used throughout the work by referring to the block diagram in Fig. 1. A baseband real input signal $x(t)$ with analog bandwidth $[-B_x, +B_x]$ is oversampled by an A/D converter and converted into the digital signal $x(nT_o)$ with sample rate f_o. The variable n identifies the integer discrete time. The interval T_o is related to the sampling frequency f_o and the signal bandwidth B_x through $f_o = \frac{1}{T_o} = 2\rho B_x$, where $\rho \geqslant 1$ is the oversampling ratio. Notice that $\rho > 1$ for oversampled signals, while $\rho = 1$ for A/D converters operating at the Nyquist frequency. The maximum digital frequency in the input signal is $f_c = \frac{B_x}{f_o} = \frac{1}{2\rho}$, meaning that the analog frequency B_x is mapped to f_c upon sampling. With this setup, the sampled signal $x(nT_o)$ at the input of the first decimation filter $H(z)$ shows frequency components in the range $[-f_c, f_c]$ as pictorially depicted in Fig. 1. The oversampling factor ρ is usually distributed between two, or more, decimation stages; therefore, it is $\rho = M \cdot \nu$ where M and ν are, respectively, the decimation factors of the first and second decimation stages.

Upon considering the sample frequency response in Fig. 1, it is worth noticing that, unlike classical filter design, the design of decimation filters imposes stringent constraints in the folding bands defined as

$$\left[\frac{p}{M} - f_c; \frac{p}{M} + f_c\right], \quad p \in \left\{1, \ldots, \left\lfloor \frac{M}{2} \right\rfloor\right\}. \tag{1}$$

On the other hand, the remaining frequency intervals, called *don't care* bands, do not require stringent selectivity since any spurious signal falling within these bands will be filtered out by the subsequent stages in the multistage decimation architecture.

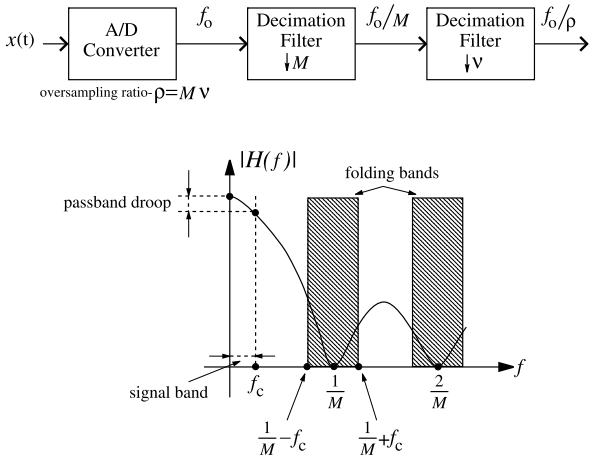

Fig. 1. Conceptual block diagram of a 2-stage decimation architecture along with a pictorial representation of the frequency response of the first decimation filter $H(z)$ and the key frequency intervals to carefully consider in the design.

2.2. The proposed decimation filters

The main goal of this paper is to introduce a new class of decimation filters for improving the magnitude response of classical comb filters while retaining their most important features, namely simple structure, low-power and multiplierless implementation. In order to meet this goal, we propose the following decimation filters with z-transfer function

$$H(z) = H_C(z) H_s(z) G\left(z^M\right). \tag{2}$$

In the previous equation, $G(z^M)$ is the z-transfer function of a passband droop-compensator filter, $H_s(z)$ is the z-transfer function of a filter used to increase folding band attenuation, and $H_C(z)$, the z-transfer function of a Kth-order comb filter decimating by M, is defined as

$$H_C(z) = \left(\frac{1}{M}\frac{1 - z^{-M}}{1 - z^{-1}}\right)^K. \tag{3}$$

The definitions of the basic building blocks $G(z^M)$ and $H_s(z)$ in (2) are derived in the next sections.

2.3. Droop-compensation filter

The main goal of filter $G(z^M)$ is to achieve passband droop compensation using an as simple as possible multiplierless filter with one free parameter independent from the decimation factor M, while working at the lower rate after decimation by M.

An effective, yet simple, compensation filter has magnitude response defined by [28]

$$\left|G\left(e^{j\omega M}\right)\right| = \left|1 + 2^{-b}\sin^2(\omega M/2)\right|, \tag{4}$$

where b is a suitable integer belonging to the set $\{-2, \ldots, 2\}$, and ω is related to the digital frequency f through the relation $\omega = 2\pi f$. Upon using the well-known trigonometric relation $\sin^2(\alpha) = [1 - \cos(2\alpha)]/2$, the z-transfer function in (4) can be rewritten as

$$G\left(z^M\right) = B\left[1 + A \cdot z^{-M} + z^{-2M}\right]. \tag{5}$$

The constant B is a scaling factor ensuring unitary gain at the digital frequency zero. It is defined in power-of-2 form as $B = -2^{-(b+2)}$, whereas $A = -[2^{b+2} + 2]$. The choice of the parameter b is discussed in the following.

2.4. Stopband improvement filter

The goal of this subfilter is to improve the attenuation of the overall filter $H(z)$ in (2) around the most critical folding band centered at the digital frequency $1/M$, using an efficient multiplierless architecture employing only two additions at lower rate.

In order to achieve this goal, we propose a cascade of two cosine filters:

$$H_s(z) = \frac{1+z^{-N_1}}{2}\,\frac{1+z^{-N_2}}{2}, \tag{6}$$

where N_1 and N_2 are two suitable integers whose choice is discussed later in the paper.

The magnitude response corresponding to (6) can be found with the substitution $z = e^{j\omega}$:

$$\left|H_s\left(e^{j\omega}\right)\right| = \left|\frac{1+e^{-j\omega N_1}}{2}\,\frac{1+e^{-j\omega N_2}}{2}\right|. \tag{7}$$

Upon recalling the Euler's relation

$$\cos\alpha = \left(e^{+j\alpha}+e^{-j\alpha}\right)/2,$$

and rewriting (7) as

$$\left|e^{-j\frac{\omega N_1}{2}}\,\frac{e^{+j\frac{\omega N_1}{2}}+e^{-j\frac{\omega N_1}{2}}}{2}\,e^{-j\frac{\omega N_2}{2}}\,\frac{e^{+j\frac{\omega N_2}{2}}+e^{-j\frac{\omega N_2}{2}}}{2}\right|, \tag{8}$$

the magnitude response of $H_s(z)$ easily follows

$$\left|H_s\left(e^{j\omega}\right)\right| = \left|\cos(\omega N_1/2)\cos(\omega N_2/2)\right|. \tag{9}$$

2.5. Transfer function of the overall filter

The transfer function of the proposed filter can be derived upon replacing (5), (6) and (3) in (2):

$$H(z) = C\left(\frac{1-z^{-M}}{1-z^{-1}}\right)^K \left(1+z^{-N_1}\right) \cdot \left(1+z^{-N_2}\right)\left[1+A\cdot z^{-M}+z^{-2M}\right], \tag{10}$$

where C, a scaling factor ensuring unitary gain at zero frequency, is defined as

$$C = \frac{-2^{-(b+4)}}{M^K}.$$

The magnitude response corresponding to (2) can be found upon substituting $z = e^{j\omega}$:

$$\left|H\left(e^{j\omega}\right)\right| = \left|\frac{1}{M^K}\,\frac{\sin^K(\omega M/2)}{\sin^K(\omega/2)}\cos(\omega N_1/2)\cos(\omega N_2/2) \cdot\left[1+2^{-b}\sin^2(\omega M/2)\right]\right|. \tag{11}$$

From the previous equation, we can notice the presence of three independent design parameters, namely b, N_1 and N_2. These parameters can be chosen given the main design parameters M and K, i.e., the decimation factor and the order of the comb filter, respectively. The choice of b, N_1 and N_2 is addressed in the next section.

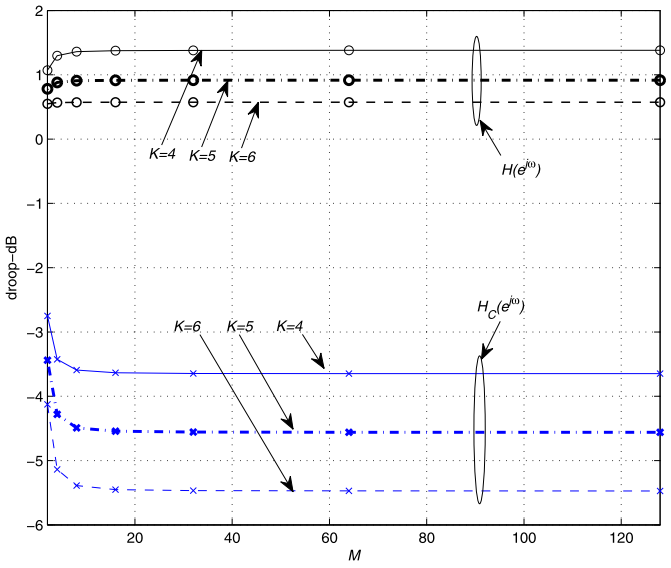

Fig. 2. Passband droop as a function of the decimation factor M for three different values of the comb order K, as noted in the legend. As far as the proposed filter is concerned, the droop is the maximum deviation from unity of (11) across the passband $[0, f_c = 1/2\rho]$. For comb filters, the droop is the frequency response evaluated at the frequency f_c. Circle-marked curves refer to the droop of the proposed filters $H(e^{j\omega})$ in (11), while the cross-marked curves refer to the droop of classical comb filters $H_C(e^{j\omega})$ in (3).

2.6. Selection of the design parameters

Choice of N_1 and N_2. Parameters N_1 and N_2 depend on the value of the decimation factor M. The main objective of the proposed filter in (6) is to increase the attenuation of a classical Kth-order comb filter across the first folding band, which is located around the frequency $1/M$ as shown in Fig. 1. Therefore, we choose N_1 and N_2 such that two additional zeros are placed in proximity of the first Kth-order zero of the comb filter in (3). We recall that the comb filter in (3) has frequency response

$$\frac{1}{M^K}\,\frac{\sin^K(\omega M/2)}{\sin^K(\omega/2)},$$

with zeros located at the digital frequencies where the numerator is zero, namely $f_p = \frac{p}{M}, \forall p \in \{1,\ldots,\lfloor\frac{M}{2}\rfloor\}$, where $\lfloor\cdot\rfloor$ is the floor of the underlined number. Given this setup, we choose N_1 and N_2 to get zeroes on the left and right side of the first comb zero at $1/M$, respectively. Depending on M, we can distinguish between the following two cases:

$$M \text{ even}: \quad N_1 = \frac{M}{2}-1; \qquad N_2 = \frac{M}{2}+1;$$
$$M \text{ odd}: \quad N_1 = \left\lfloor\frac{M}{2}\right\rfloor; \qquad N_2 = N_1+1. \tag{12}$$

Choice of b. The design parameter b depends on both K and the decimation factor ν of the stage that follows the first decimator by M, while it is very weakly dependent on M. To clarify the latter statement, Fig. 2 shows the droop of the proposed filters $H(e^{j\omega})$ in (11) as a function of the decimation factor M for three sample values of K. As far as the proposed filter is concerned, the droop is the maximum deviation from unity of (11) across the passband $[0, f_c = 1/2\rho]$. For comb filters, the droop is the frequency response evaluated at the frequency f_c.

Fig. 2 clearly shows the weak dependence of the droop against M, and the improvement guaranteed by the proposed filters compared to classical comb filters.

Table 1
Values of b for $M = 16$ and ν as noted in each column.

K	$\nu = 2$	$\nu = 3$	$\nu > 3$
1	$b = 1$	$b = 1$	$b = 1$
2	$b = 0$	$b = 1$	$b = 1$
3	$b = 0$	$b = 0$	$b = 0$
4	$b = -1$	$b = 0$	$b = 0$
5	$b = -1$	$b = 0$	$b = 0$
6	$b = -1$	$b = -1$	$b = 0$

The decimation factor ν determines the passband width and the folding bands. We used a MATLAB program to exhaustively search for the best values of b minimizing the passband distortion of the overall filter (11) for any given M, K and ν. The values of b for $M = 16$ and various values of ν are shown in Table 1.

Before concluding this section, we would like to point out that the stopband response of the proposed filter (11) can be improved by cascading more cosine filters in the z-transfer function (6) and upon choosing the corresponding parameters N_1 and N_2 in order to have zeros in the first folding band centered on $1/M$. However, this extension comes with an increased computational complexity of the overall structure.

3. Magnitude response of the proposed filters

In this section we show several filter frequency responses for the sake of contrasting the magnitude response of the proposed class of decimation filters in (11) to the magnitude response of classical comb filters in (3).

In the first design example we consider a decimation factor $M = 16$ and an oversampling factor $\rho = 32$. This example is typical of moderately oversampled signals. The normalized bandwidth of the sampled signal is $f_c = \frac{1}{2\rho} = 0.0156$. This means that the analog bandwidth B_x of the analog signal $x(t)$ is mapped to the digital frequency interval $[-0.0156, +0.0156]$ after A/D conversion with sample rate f_o. The first folding band (from (1) using $p = 1$) is

$$\left[\frac{1}{M} - f_c = 0.0469, \frac{1}{M} + f_c = 0.0781\right].$$

Let us discuss the design steps of the proposed decimation filter.

1. Given $M = 16$, from (12) it is $N_1 = 7$ and $N_2 = 9$.
2. Considering $K = 5$ and $\nu = 2$, from Table 1 we find $b = -1$.

Fig. 3 compares the magnitude responses of the proposed filter $H(e^{j2\pi f})$ with that of a 5th-order comb filter ($K = 5$ and $M = 16$ in (3)) across the digital frequency interval $[0, 0.5]$. A key observation here is that the magnitude response of the proposed filters lies beneath the magnitude response of comb filters in the folding bands, especially in the first one. This behavior can be clearly seen in the rightmost plot of Fig. 4 around the first folding band: the continuous curve, which is the magnitude response of the proposed filter, falls below the magnitude response of the comb filter thus yielding a much greater spurious signal rejection around the considered folding band.

The passband behavior of the proposed filter $H(e^{j2\pi f})$ is compared to the one of a classical 5th-order comb filter in the leftmost plot of Fig. 4. Notice that the proposed filter introduces a maximum droop of 0.9 dB, while the 5th-order comb filter presents a signal distortion as high as 4.5 dB at $f_c = 0.0156$. The latter value must be compensated by the FIR filter following the comb filter in the multistage decimation chain, thus increasing the computational complexity of the overall decimation architecture.

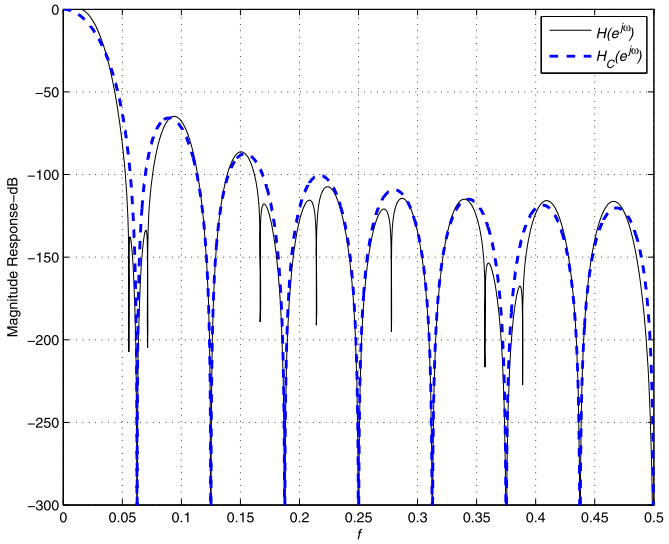

Fig. 3. Magnitude responses (in dB) of the proposed filter $H(e^{j2\pi f})$ (solid curve) and of a classical comb filter (dashed curve) for the following set of design parameters: $M = 16$, $K = 5$, $b = -1$, $N_1 = 7$, $N_2 = 9$, $\nu = 2$.

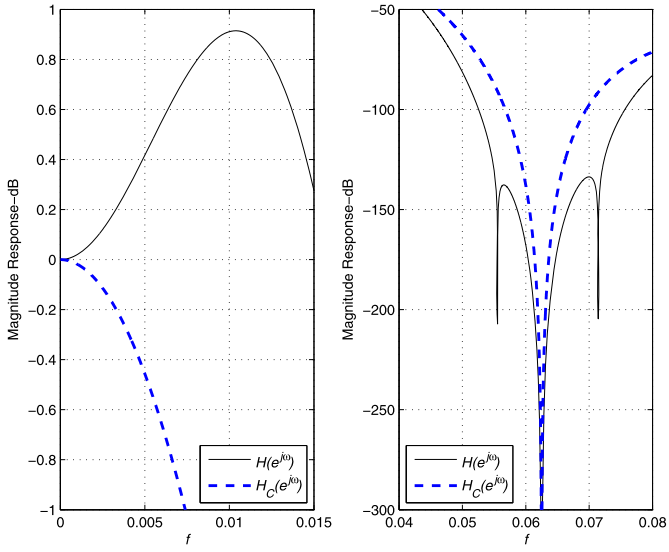

Fig. 4. Magnitude responses (in dB) of the proposed filter $H(e^{j2\pi f})$ (solid curve) and of a classical comb filter (dashed curve). The leftmost plot shows the magnitude response behavior at baseband, whereas the rightmost plot highlights the response around the first folding band. In all subplots, the set of design parameters is as follows: $M = 16$, $K = 5$, $b = -1$, $N_1 = 7$, $N_2 = 9$, $\nu = 2$.

In the second design example we consider a decimation factor $M = 32$ and an oversampling factor $\rho = 64$. This example is typical of highly oversampled signals. The normalized bandwidth of the sampled signal is $f_c = \frac{1}{2\rho} = 0.0078125$, while the first folding band (from (1) with $p = 1$) is

$$\left[\frac{1}{M} - f_c = 0.0234375, \frac{1}{M} + f_c = 0.0390625\right].$$

Let us discuss the design steps of the proposed decimation filter.

1. Given $M = 32$, from (12) it is $N_1 = 15$ and $N_2 = 17$.
2. Considering $K = 5$ and $\nu = 2$, from Table 1 we find $b = -1$. As pointed put in a previous section, the values of b can be considered as independent of the values of the decimation factor M.

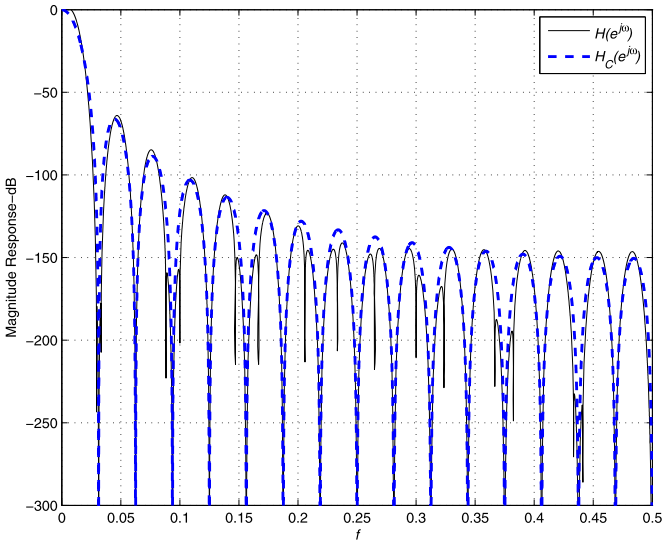

Fig. 5. Magnitude responses (in dB) of the proposed filter $H(e^{j2\pi f})$ (solid curve) and of a classical comb filter (dashed curve) for the following set of design parameters: $M = 32$, $K = 5$, $b = -1$, $N_1 = 15$, $N_2 = 17$, $\nu = 2$.

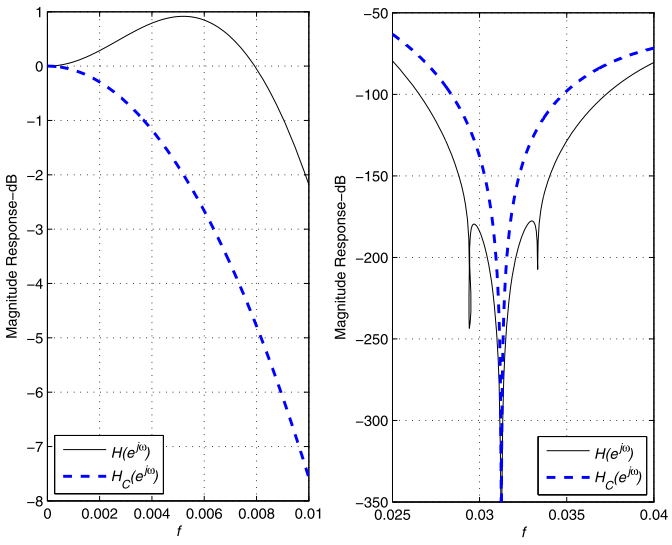

Fig. 6. Magnitude responses (in dB) of the proposed filter $H(e^{j2\pi f})$ (solid curve) and of a classical comb filter (dashed curve). The leftmost plot shows the magnitude response behavior at baseband, whereas the rightmost plot highlights the response around the first folding band. In all subplots, the set of design parameters is as follows: $M = 32$, $K = 5$, $b = -1$, $N_1 = 15$, $N_2 = 17$, $\nu = 2$.

Fig. 5 compares the magnitude responses of the proposed filter $H(e^{j2\pi f})$ with that of a 5th-order comb filter ($K = 5$ and $M = 32$ in (3)) across the digital frequency interval $[0, 0.5]$. As already noticed in the previous design case, the magnitude response of the proposed filters lies beneath the magnitude response of comb filters in the folding bands. This behavior is confirmed by the rightmost plot of Fig. 6 that shows the frequency responses around the first folding band.

The passband behavior of the proposed filter $H(e^{j2\pi f})$ is compared to the one of a classical 5th-order comb filter in the leftmost plot of Fig. 6. Notice that the proposed filter introduces a maximum droop of 0.9 dB, while the 5th-order comb filter presents a signal distortion of about 5 dB at $f_c = 0.0078125$.

In the next example we consider odd values of the decimation factor M.

To get started, let us consider the case $M = 15$ and oversampling factor $\rho = 30$. The normalized bandwidth of the sampled

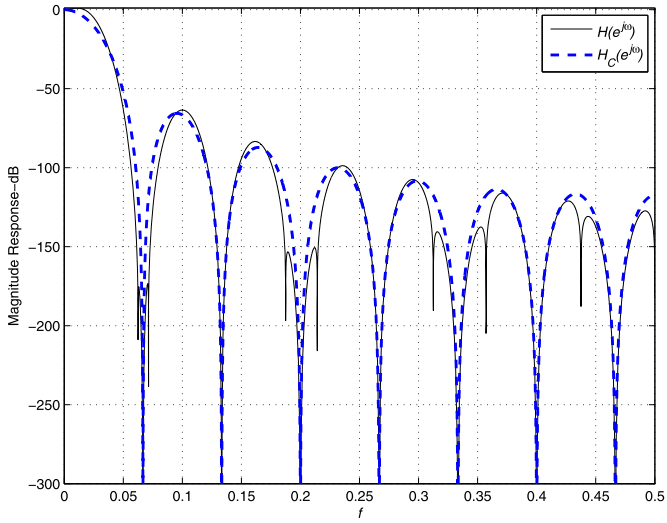

Fig. 7. Magnitude responses (in dB) of the proposed filter $H(e^{j2\pi f})$ (solid curve) and of a classical comb filter (dashed curve) for the following set of design parameters: $M = 15$, $K = 5$, $b = -1$, $N_1 = 7$, $N_2 = 8$, $\nu = 2$.

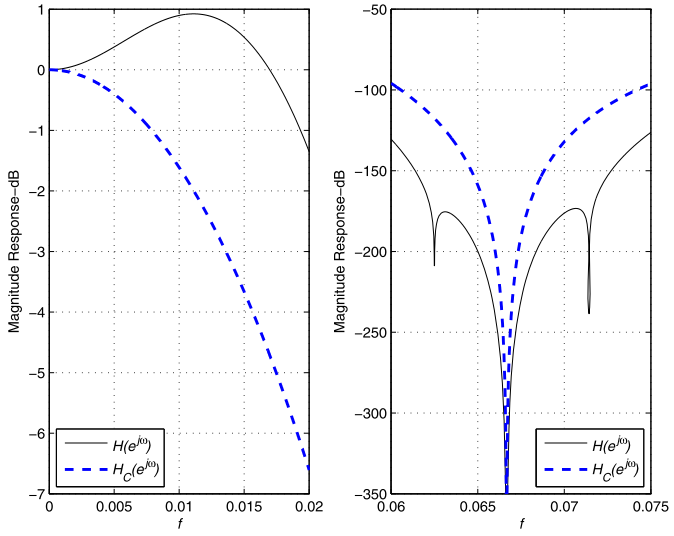

Fig. 8. Magnitude responses (in dB) of the proposed filter $H(e^{j2\pi f})$ (solid curve) and of a classical comb filter (dashed curve). The leftmost plot shows the magnitude response behavior at baseband, whereas the rightmost plot highlights the response around the first folding band. In all subplots, the set of design parameters is as follows: $M = 15$, $K = 5$, $b = -1$, $N_1 = 7$, $N_2 = 8$, $\nu = 2$.

signal is $f_c = \frac{1}{2\rho} = 0.0166$, while the first folding band (from (1) with $p = 1$) is

$$\left[\frac{1}{M} - f_c = 0.05, \frac{1}{M} + f_c = 0.0833\right].$$

Let us discuss the design steps of the proposed decimation filter.

1. Given $M = 15$, from (12) it is $N_1 = 7$ and $N_2 = 8$.
2. Considering $K = 5$ and $\nu = 2$, from Table 1 we find $b = -1$.

Fig. 7 compares the magnitude responses of the proposed filter $H(e^{j2\pi f})$ with that of a 5th-order comb filter ($K = 5$ and $M = 15$ in (3)) over the frequency interval $[0, 0.5]$. Similarly to the previous examples, the magnitude response of the proposed filters lies below the magnitude response of comb filters in the folding bands.

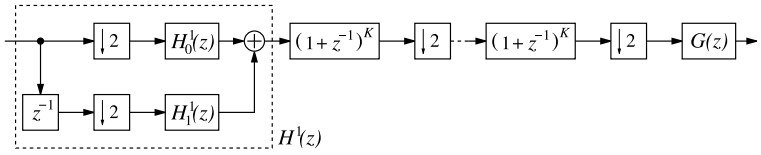

Fig. 9. Architecture of a non-recursive implementation of decimation filter $H(z)$ in (10) for $M = 2^r$. The first stage implements the z-transfer function derived in (18) while the other $r-1$ stages represent the remaining products in the decomposition (13). The last stage implements the droop compensator with z-transfer function $G(z)$.

This behavior can be clearly seen in the rightmost plot of Fig. 8 around the first folding band.

The passband behavior of the proposed filter $H(e^{j2\pi f})$ is compared to the one of a classical 5th-order comb filter in the leftmost plot of Fig. 8. Notice that the proposed filter introduces a maximum droop of 0.9 dB, while the 5th-order comb filter presents a signal distortion of about 4 dB at $f_c = 0.0166$. A common observation from all these design examples is that the passband distortions of the proposed filters do not exceed 0.9 dB regardless of the chosen set of parameters, and it compares favorably to the distortion of comb filters, which is always greater than 4 dB across all the possible choices of the design parameters.

To summarize the main observations derived from these design examples, we can say that 1) the proposed filters show improved magnitude response behavior in both passband and folding bands; 2) better passband distortion compensation (for $\nu = 2$) is obtained for higher values of K; 3) good droop compensation is obtained for all K when narrow signal bandwidths are considered, i.e., for higher oversampling factors ρ.

4. Efficient architectures and implementations issues

In this section we present efficient architectures for implementing the proposed filters depending on the expression of the decimation factor M.

4.1. Efficient structure for $M = 2^p$

When M can be represented as a suitable power-of-2 integer, say $M = 2^r$, with r a positive integer, the z-transfer function in (10) can be implemented by exploiting the following formula

$$\left(\frac{1-z^{-M}}{1-z^{-1}}\right)^K = \prod_{i=0}^{\log_2(M)-1} \left(1+z^{-2^i}\right)^K. \tag{13}$$

By applying the commutative property of multirate theory [12], this architecture presents $r = \log_2 M$ stages of filtering with z-transfer function $(1+z^{-1})^K$ whereby the ith stage operates at the reduced sample rate $f_o/2^{i-1}$ with f_o being the sampling data rate at the input. The first stage of the decimation chain has z-transfer function

$$H^1(z) = \left(1+z^{-1}\right)^K \cdot \left(1+z^{-N_1}\right) \cdot \left(1+z^{-N_2}\right), \tag{14}$$

while the last stage is the droop-compensation filter $G(z) = B[1 + A \cdot z^{-1} + z^{-2}]$. We briefly notice that $G(z)$ is obtained from multirate identities by moving $G(z^M)$ in (10) through the decimator by M.

Considering the expressions of N_1 and N_2 in (12) for M even, the z-transfer function in (14) can be rewritten as

$$H^1(z) = \left(1+z^{-1}\right)^K \cdot \left(1+z^{-\frac{M}{2}+1}\right) \cdot \left(1+z^{-\frac{M}{2}-1}\right). \tag{15}$$

In order to reduce power consumption, which depends on the sampling data rate, we apply polyphase decomposition at each stage so as to move filtering at lower rate. First, we polyphase decompose $(1+z^{-1})^K$ as follows

$$\left(1+z^{-1}\right)^K = H_0\left(z^2\right) + z^{-1}H_1\left(z^2\right), \tag{16}$$

where $H_0(z)$ and $H_1(z)$ are the polyphase components. Then, we rewrite $(1+z^{-\frac{M}{2}+1}) \cdot (1+z^{-\frac{M}{2}-1})$ in (15) as:

$$\begin{aligned}\left(1+z^{-\frac{M}{2}+1}\right) \cdot \left(1+z^{-\frac{M}{2}-1}\right) &= \left(1+z^{-M}\right) + z^{-1}\left(z^{-\frac{M}{2}+2} + z^{-\frac{M}{2}}\right) \\ &= H_{S0}\left(z^2\right) + z^{-1}H_{S1}\left(z^2\right),\end{aligned} \tag{17}$$

where $H_{S0}(z^2) = 1 + z^{-M}$ and $H_{S1}(z^2) = z^{-\frac{M}{2}+2} + z^{-\frac{M}{2}}$.

Upon combining (16) and (17), (15) can be rewritten as

$$\begin{aligned}H^1(z) &= \left(H_0\left(z^2\right) + z^{-1}H_1\left(z^2\right)\right)\left(H_{S0}\left(z^2\right) + z^{-1}H_{S1}\left(z^2\right)\right) \\ &= H_0^1\left(z^2\right) + z^{-1}H_1^1\left(z^2\right),\end{aligned} \tag{18}$$

with

$$\begin{aligned}H_0^1\left(z^2\right) &= H_{S0}\left(z^2\right)H_0\left(z^2\right) + z^{-2}H_{S1}\left(z^2\right)H_1\left(z^2\right), \\ H_1^1\left(z^2\right) &= H_{S1}\left(z^2\right)H_0\left(z^2\right) + H_{S0}\left(z^2\right)H_1\left(z^2\right).\end{aligned} \tag{19}$$

Using multirate identities [7], the decimation filter $H(z)$ in (10) can be realized using the architecture in Fig. 9.

Some observations are in order. Concerning the decimation architecture in Fig. 9, we notice that 1) it does not present any overflow problem since it is intrinsically non-recursive; 2) it does not accomplish filtering at the high input data rate; 3) it does not contain any multiplier thus representing a very effective implementation for applications where low-power consumption and reduced VLSI area are foremost; 4) it is reconfigurable: for given K and decimation factor M the architecture in Fig. 9 presents $\log_2 M$ identical stages of decimation (each stage requires K additions), while the first stage $H^1(z)$[1] and the last one $G(z)$ are the same regardless of $\log_2 M$ as long as $\log_2 M \geqslant 1$. We note that $G(z)$ requires two additions at the lowest rate in the decimation chain.

To clarify the derivations above, we discuss some design examples using specific parameters.

Example 1. Let us consider the non-recursive architecture in Fig. 9 for the following set of parameters: $M = 32$, $K = 4$, and $b = 0$.

When $M = 32$, from (12) it is $N_1 = 15$, $N_2 = 17$ and $r = \log_2 32 = 5$. Therefore, the architecture contains 5 stages of decimation by 2.

From (17), we have

$$\begin{aligned}H_{S0}\left(z^2\right) &= 1 + z^{-32} \quad \Rightarrow \quad H_{S0}(z) = 1 + z^{-16}, \\ H_{S1}\left(z^2\right) &= z^{-16} + z^{-18} \quad \Rightarrow \quad H_{S1}(z) = z^{-8} + z^{-9}.\end{aligned} \tag{20}$$

From (16), we have the following polyphase decomposition

$$\begin{aligned}\left(1+z^{-1}\right)^4 &= 1 + 4z^{-1} + 6z^{-2} + 4z^{-3} + z^{-4} \\ &= \left(1 + 6z^{-2} + z^{-4}\right) + z^{-1}\left(4 + 4z^{-2}\right).\end{aligned} \tag{21}$$

Therefore, it is

[1] We notice that, depending on M, there may be different delays in $H_{S0}(z)$ and $H_{S1}(z)$.

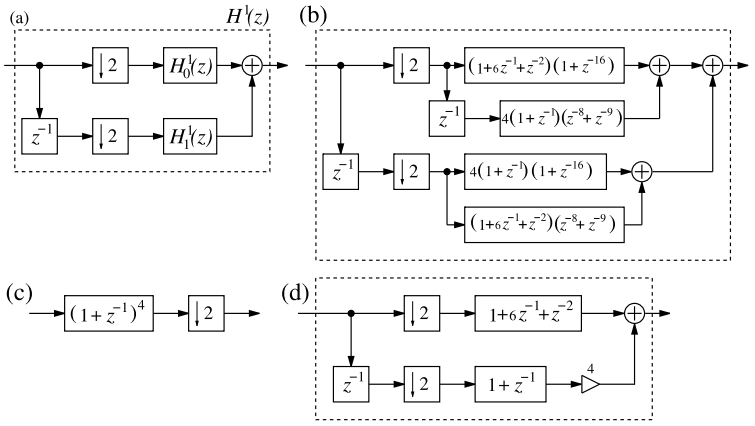

Fig. 10. (a) Architecture of the first filter cell $H^1(z)$ considered in Example 1, and (b) polyphase implementation in (18) obtained upon replacing the subfilters (20) and (22) in (19). (c) Basic decimation stage by 2 implementing the z-transfer function in (21) of Example 1 for $K=4$ and $M=32$, and (d) polyphase implementation as detailed in (21).

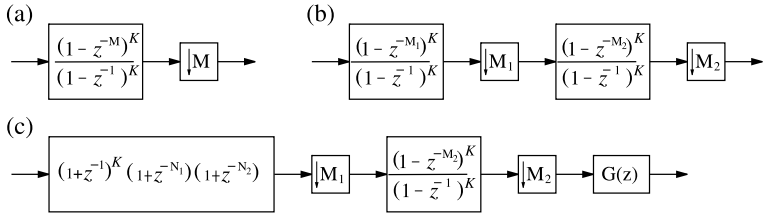

Fig. 11. (a) z-transfer function considered in (23), and (b) two-stage architecture resulting from the use of multirate identities. (c) Two-stage architecture for implementing the proposed decimation filter for the case $M=M_1\cdot M_2=2M_2$.

$$H_0(z^2)=1+6z^{-2}+z^{-4} \quad \Rightarrow \quad H_0(z)=1+6z^{-1}+z^{-2},$$
$$H_1(z^2)=4+4z^{-2} \quad \Rightarrow \quad H_1(z)=4+4z^{-1}. \tag{22}$$

With this setup, the first stage $H^1(z)$ of the decimation architecture in Fig. 10(a) can be polyphase decomposed as in Fig. 10(b). The other four stages of decimation by 2 in Fig. 10(c) can be implemented using polyphase decomposition as depicted in Fig. 10(d).

4.2. Efficient structure for $M=M_1M_2$

In this section we address the design of efficient structures when the decimation factor M can be decomposed into the product of two integers M_1 and M_2. Moreover, we distinguish between the two cases M even where we consider $M_1=2$, and M odd where we assume $M_1\leqslant M_2$.

First of all, notice that for $M=M_1M_2$, the comb section in (10), which is depicted in Fig. 11(a), can be decomposed as

$$\left(\frac{1-z^{-M}}{1-z^{-1}}\right)^K=\left(\frac{1-z^{-M_1M_2}}{1-z^{-M_1}}\right)^K\left(\frac{1-z^{-M_1}}{1-z^{-1}}\right)^K. \tag{23}$$

Then, it can be implemented as depicted in Fig. 11(b) upon using multirate identities [12].

For $M_1=2$, the first stage $H^1(z)$ has the same z-transfer function and practical implementation as detailed in (18). In this case, we can use the following relation to reduce the number of addition to one:

$$\frac{1-z^{-2}}{1-z^{-1}}=1+z^{-1}. \tag{24}$$

Therefore, the two-stage architecture in Fig. 11(b) particularizes to the one shown in Fig. 11(c). From Fig. 11(c) we notice that the first filter before the decimation by M_1 requires $K+2$ additions, while the second filter after the decimation by M_1 requires $2K$ additions.

For M odd, the filter in the first stage can be realized using the following polyphase decomposition:

$$H^1(z)=\left(\frac{1-z^{-M_1}}{1-z^{-1}}\right)^K\left(1+z^{-N_1}\right)\cdot\left(1+z^{-N_2}\right)$$
$$=\sum_{\lambda=0}^{M_1-1}z^{-\lambda}H_\lambda^1\left(z^{M_1}\right). \tag{25}$$

Concerning the second stage, regardless of M (even or odd) we can resort to the following polyphase decomposition

$$\left(\frac{1-z^{-M_2}}{1-z^{-1}}\right)^K=\sum_{\lambda=0}^{M_2-1}z^{-\lambda}H_\lambda^2\left(z^{M_2}\right). \tag{26}$$

To understand the use of these derivations, we discuss two examples.

Example 2. Let us consider the following set of parameters: $M=10$, $M_1=2$, $M_2=5$, $N_1=4$, $N_2=6$, $K=3$, and $b=0$. With this setup and recalling (24), the first stage $H^1(z)$ can be written as:

$$H^1(z)=\left(\frac{1-z^{-M_1}}{1-z^{-1}}\right)^K\left(1+z^{-N_1}\right)\cdot\left(1+z^{-N_2}\right)$$
$$=\left(\frac{1-z^{-2}}{1-z^{-1}}\right)^3\left(1+z^{-4}\right)\cdot\left(1+z^{-6}\right)$$
$$=\left(1+z^{-1}\right)^3\left(1+z^{-4}\right)\cdot\left(1+z^{-6}\right). \tag{27}$$

The z-transfer function $(1+z^{-1})^3$ can be polyphase decomposed as:

$$\left(1+z^{-1}\right)^3=\left(1+3z^{-1}+3z^{-2}+z^{-3}\right)$$
$$=H_0\left(z^2\right)+z^{-1}H_1\left(z^2\right),$$

$$H_0(z^2) = 1 + 3z^{-2} \quad \rightarrow \quad H_0(z) = 1 + 3z^{-1},$$
$$H_1(z^2) = 3 + z^{-2} \quad \rightarrow \quad H_1(z) = 3 + z^{-1}. \tag{28}$$

The z-transfer function $(1+z^{-4})\cdot(1+z^{-6})$ can be decomposed as:

$$\begin{aligned}(1+z^{-4})\cdot(1+z^{-6}) &= (1+z^{-4}+z^{-6}+z^{-10}) \\ &= H_{S0}(z^2) + z^{-1}H_{S1}(z^2),\end{aligned} \tag{29}$$

where $H_{S0}(z^2) = (1+z^{-4}+z^{-6}+z^{-10})$ and $H_{S1}(z^2) = 0$.

The polyphase components of the second stage can be found upon using (26):

$$H_0^2(z^5) = 1 + 18z^{-5} + z^{-10}, \qquad H_1^2(z^5) = 3 + 15z^{-5},$$
$$H_2^2(z^5) = 6 + 10z^{-5}, \qquad H_3^2(z^5) = 10 + 6z^{-5},$$
$$H_4^2(z^5) = 15 + 3z^{-5},$$
$$H_0^2(z) = 1 + 18z^{-1} + z^{-2}, \qquad H_1^2(z) = 3 + 15z^{-1},$$
$$H_2^2(z) = 6 + 10z^{-1}, \qquad H_3^2(z) = 10 + 6z^{-1},$$
$$H_4^2(z) = 15 + 3z^{-1}. \tag{30}$$

A very efficient implementation of the second stage with z-transfer function $H^2(z)$ given by

$$\begin{aligned}H^2(z) &= H_0^2(z^5) + z^{-1}H_1^2(z^5) + z^{-2}H_2^2(z^5) \\ &\quad + z^{-3}H_3^2(z^5) + z^{-4}H_4^2(z^5)\end{aligned} \tag{31}$$

is shown in Fig. 12. In this architecture, each polyphase component $H_\lambda^2(z)$ has been optimized by first decomposing each integer coefficient as the summation of power-of-two coefficients, and then by employing coefficient sharing arguments. As an example, the first two polyphase components can be rewritten as

$$H_0^2(z) = 1 + 18z^{-1} + z^{-2} = 1 + z^{-1}\left[z^{-1} + \left(2^4 + 2^1\right)\right],$$
$$H_1^2(z) = 3 + 15z^{-1} = \left(2^1 + 2^0\right)\left[1 + \left(2^2 + 2^0\right)z^{-1}\right], \tag{32}$$

and implemented as in Fig. 12. We notice in passing that these implementations feature minimum number of shift registers.

The droop compensator at the end of the decimation chain has z-transfer function $G(z) = 1 - 6z^{-1} + z^{-2}$.

Example 3. Let us consider the following set of parameters: $M = 9$, $M_1 = 3$, $M_2 = 3$, $N_1 = 4$, $N_2 = 5$, $K = 3$, and $b = 0$. With this setup, the polyphase components of the first stage $H^1(z)$ can be written as:

$$H_0^1(z^3) = 1 + 7z^{-3} + 10z^{-6} + 10z^{-9} + 7z^{-12} + z^{-15},$$
$$H_1^1(z^3) = 3 + 7z^{-3} + 13z^{-6} + 7z^{-9} + 6z^{-12},$$
$$H_2^1(z^3) = 6 + 7z^{-3} + 13z^{-6} + 7z^{-9} + 3z^{-12},$$
$$H_0^1(z) = 1 + 7z^{-1} + 10z^{-2} + 10z^{-3} + 7z^{-4} + z^{-5},$$
$$H_1^1(z) = 3 + 7z^{-1} + 13z^{-2} + 7z^{-3} + 6z^{-4},$$
$$H_2^1(z) = 6 + 7z^{-1} + 13z^{-2} + 7z^{-3} + 3z^{-4}, \tag{33}$$

whereas the polyphase components of the second stage $H^2(z)$ can be written as:

$$H_0^2(z^3) = 1 + 7z^{-3} + z^{-6},$$
$$H_1^2(z^3) = 3 + 6z^{-3},$$
$$H_2^2(z^3) = 6 + 3z^{-3},$$
$$H_0^2(z) = 1 + 7z^{-1} + z^{-2},$$
$$H_1^2(z) = 3 + 6z^{-1},$$
$$H_2^2(z) = 6 + 3z^{-1}. \tag{34}$$

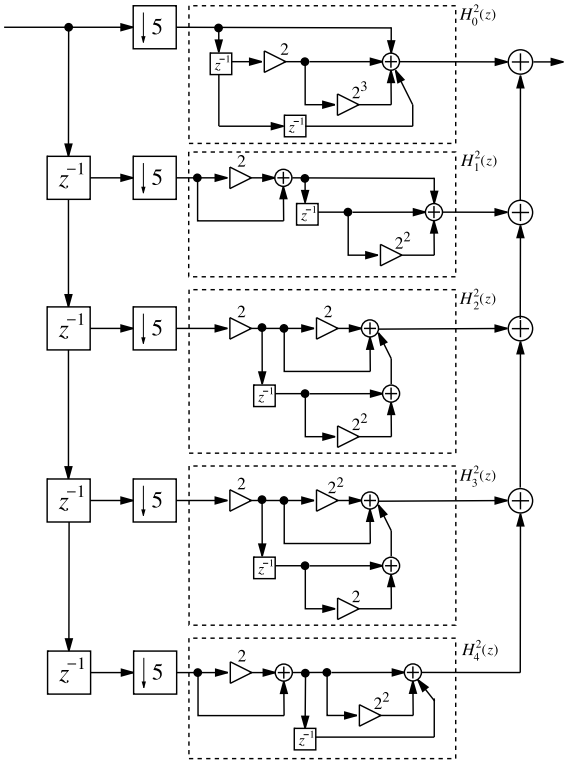

Fig. 12. Efficient implementation of the 2nd decimation stage in Example 2 using the polyphase decomposition in (26) along with the polyphase components $H_\lambda^2(z)$, with $\lambda \in \{0, \ldots, 4\}$.

The droop compensator at the end of the decimation chain has z-transfer function $G(z) = 1 - 6z^{-1} + z^{-2}$.

4.3. Efficient structure for M a prime number

When the decimation factor M is a prime number, the most efficient architecture consists in the polyphase decomposition of the filter $H(z)$:

$$\begin{aligned}H(z) &= \left(\frac{1-z^{-M}}{1-z^{-1}}\right)^K \left(1+z^{-N_1}\right)\cdot\left(1+z^{-N_2}\right) \\ &= \sum_{\lambda=0}^{M-1} z^{-\lambda} H_\lambda^1(z^M).\end{aligned} \tag{35}$$

The polyphase components can be found and implemented using the same approach of the previous examples.

5. Comparisons

In this section we compare the class of filters addressed in this work with three techniques proposed in the literature. The goal is to highlight the improved performance in terms of spurious signal rejection around the folding bands compared to state-of-the-art techniques.

The first comparison is with the sharpening method proposed in [22] for which we choose a decimation factor $M = 20$ and residual decimation factor $\nu = 8$ so as to have $\rho = 160$. The sharpening polynomial proposed in [22] is $3H^2(z) - 2H^3(z)$ where $H(z)$ is the z-transfer function of the basic comb filter used for sharpening.

In the method proposed in this work, the comb filter is cascaded twice and the design parameters are as follows: $N_1 = 9$, $N_2 = 11$ and $b = 1$. The magnitude responses of the two filters are compared in Fig. 13 versus the frequency axis. From this figure we

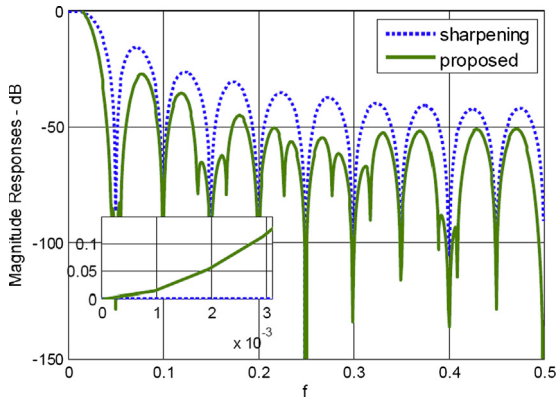

Fig. 13. Magnitude responses (in dB) of the sharpened filter proposed in [22] (dotted curve labeled sharpening) and of the proposed filter (continuous curve labeled proposed) for the following set of design parameters: $M = 20$, $\nu = 8$, $N_1 = 9$, $N_2 = 11$ and $b = 1$.

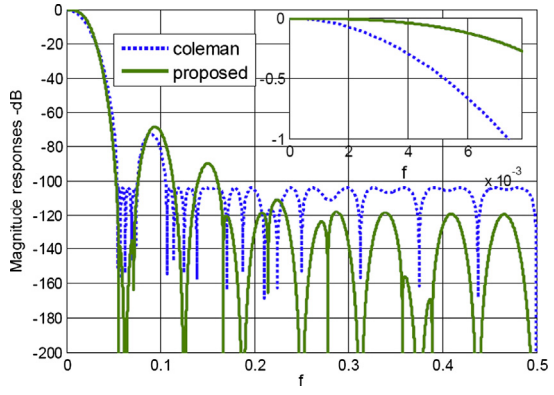

Fig. 14. Magnitude responses (in dB) of the filter proposed in [31] (dotted curve labeled coleman) and of the proposed filter (continuous curve labeled proposed) for the following set of design parameters: $M = 16$, $\nu = 4$, $N_1 = 7$, $N_2 = 9$ and $b = 0$.

observe that the proposed method presents better alias rejection across the folding bands, while the sharpening method has better passband characteristic over a wider frequency range. From a computational point of view, however, the proposed structure does not have filtering at high input rate thus resulting in more computationally efficient architecture.

The second comparison is with the recent proposal in [31] where a 5th degree Chebyshev polynomial $T_5(x) = 5x - 20x^2 + 16x^5$ is used. For comparison, we consider $M = 16$ and residual decimation factor $\nu = 4$. Upon using the proposed method, the number of the cascaded comb filters is 5, while other parameters are as follows: $N_1 = 7$, $N_2 = 9$, and $b = 0$. The magnitude responses of these two filters are contrasted in Fig. 14. From this figure we notice the improved passband behavior of the proposed class of filters. Moreover, the proposed method provides more attenuation in the folding bands thus resulting in better spurious signal rejection around the folding bands. However, the advantage of the Coleman's method is that all folding bands have controlled width and the same controlled attenuations.

The last comparison is with the results of a companion work recently published in this journal [19]. For simplicity, we will use the acronim TSNGCF short for Two-Stage Non-recursive Generalized Comb Filter, to refer to the method [19].

The proposed method here is compared to the filter in design Example 1 [19] where the parameters are as follows: decimation factor $M = 16$, oversampling factor $\rho = 64$, $M_1 = 8$, $N = 3$, $b = 0$, $I = 15$, and $k = 4$. In the proposed method, we have $N_1 = 7$, $N_2 = 9$, $b = 0$, and the comb filter is cascaded five times. The magnitude responses are shown in Fig. 15. We notice in passing that

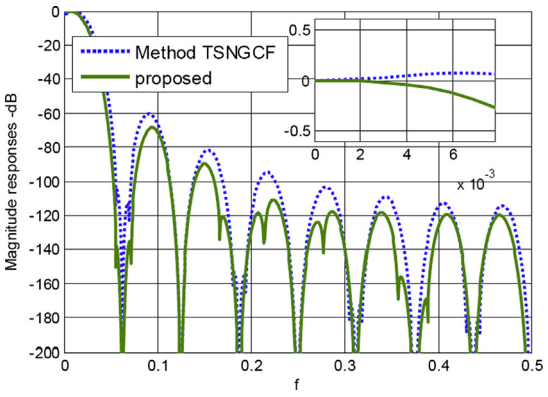

Fig. 15. Magnitude responses (in dB) of the filter proposed in [19] (dotted curve labeled Method TSNGCF) and of the proposed filter (continuous curve labeled proposed) for the following set of design parameters: $M = 16$, $\nu = 4$, $N_1 = 7$, $N_2 = 9$ and $b = 0$.

the attenuation in the first folding band is better in the filter designed with the proposed method, while in other folding bands are similar. However, method TSNGCF presents wider passband range.

6. Conclusion

This paper proposed a class of low-complexity, reconfigurable decimation filters suitable for decimating oversampled discrete-time signals. The proposed filters improve greatly the frequency response of classical comb filters by introducing extra-attenuation around the so-called folding bands and by reducing the passband distortion via an effective droop-compensator block.

Like comb filters, the proposed class can be realized through multiplierless architectures, which are also discussed thoroughly in the paper. Unlike comb filters, the proposed filters have superior spurious signal rejection and a greatly reduced droop in the signal passband. These features make the proposed filters suitable for multistage decimation applications, such as digital down-converters, as well as for decimating oversampled digital signals as produced by $\Sigma\Delta$ A/D converters.

Design examples, design hints, and several implementation architectures were also discussed to point out the main features of the proposed class of decimation filters. Moreover, comparisons with other works in the very recent literature point out the improved performance guaranteed by the proposed class of filters in terms of spurious signal rejection around the folding bands.

References

[1] M. Laddomada, F. Daneshgaran, M. Mondin, R.M. Hickling, A PC-based software receiver using a novel front–end technology, IEEE Commun. Mag. 39 (8) (August 2001) 136–145.
[2] F. Daneshgaran, M. Laddomada, Transceiver front–end technology for software radio implementation of wideband satellite communication systems, Wirel. Pers. Commun. 24 (12) (December 2002) 99–121.
[3] J. Mitola, The software radio architecture, IEEE Commun. Mag. 33 (5) (May 1995) 26–38.
[4] J.H. Reed, Software Radio: A Modern Approach to Radio Engineering, Prentice Hall PTR, 2002.
[5] T. Hentschel, G. Fettweis, Sample rate conversion for software radio, IEEE Commun. Mag. 38 (8) (August 2000) 142–150.
[6] R.E. Crochiere, L.R. Rabiner, Multirate Digital Signal Processing, Prentice Hall PTR, 1983.
[7] P.P. Vaidyanathan, Multirate digital filters, filter banks, polyphase networks, and applications: A tutorial, Proc. IEEE 78 (1) (January 1990) 56–93.
[8] S.R. Norsworthy, R. Schreier, G.C. Temes, Delta–Sigma Data Converters: Theory, Design, and Simulation, IEEE Press, 1997.
[9] G. Jovanovic-Dolecek, Introduction to multirate systems, in: Multirate Systems: Design and Application, Idea Group Publishing, Hershey, USA, 2002, Chapter 1.

[10] F. Harris, Multirate Signal Processing for Communications, Prentice Hall PTR, 2004.
[11] E.B. Hogenauer, An economical class of digital filters for decimation and interpolation, IEEE Trans. Acoust. Speech Signal Process. ASSP-29 (2) (April 1981) 155–162.
[12] S. Chu, C.S. Burrus, Multirate filter designs using comb filters, IEEE Trans. Circuits Syst. CAS-31 (November 1984) 913–924.
[13] M. Laddomada, Design of multistage decimation filters using cyclotomic polynomials: Optimization and design issues, IEEE Trans. Circuits Syst. I 55 (7) (August 2008) 1977–1987.
[14] M. Laddomada, D.E. Troncoso, G. Jovanovic-Dolecek, Design of multiplierless decimation filters using an extended search of cyclotomic polynomials, IEEE Trans. Circuits Syst. II. Express Briefs 58 (2) (February 2011) 115–119.
[15] L. Lo Presti, Efficient modified-sinc filters for sigma–delta A/D converters, IEEE Trans. Circuits Syst. II 47 (11) (November 2000) 1204–1213.
[16] M. Laddomada, Generalized comb decimation filters for $\Sigma\Delta$ A/D converters: Analysis and design, IEEE Trans. Circuits Syst. I 54 (5) (May 2007) 994–1005.
[17] M. Laddomada, On the polyphase decomposition for design of generalized comb decimation filters, IEEE Trans. Circuits Syst. I 55 (8) (September 2008) 2287–2299.
[18] G.J. Dolecek, M. Laddomada, An economical class of droop-compensated generalized comb filters: Analysis and design, IEEE Trans. Circuits Syst. II 57 (4) (April 2010) 275–279.
[19] G.J. Dolecek, M. Laddomada, A novel two-stage nonrecursive architecture for the design of generalized comb filters, Digital Signal Process. 22 (5) (September 2012) 859–868.
[20] H. Aboushady, Y. Dumonteix, M. Louërat, H. Mehrez, Efficient polyphase decomposition of comb decimation filters in $\Sigma\Delta$ analog-to-digital converters, IEEE Trans. Circuits Syst. II. Analog Digital Signal Process. 48 (10) (October 2001) 898–903.
[21] J. Kaiser, R. Hamming, Sharpening the response of a symmetric nonrecursive filter by multiple use of the same filter, IEEE Trans. Acoust. Speech Signal Process. ASSP-25 (October 1977) 415–422.
[22] A.Y. Kwentus, Z. Jiang, A.N. Willson Jr., Application of filter sharpening to cascaded integrator-comb decimation filters, IEEE Trans. Signal Process. 45 (2) (February 1997) 457–467.
[23] M. Laddomada, Comb-based decimation filters for $\Sigma\Delta$ A/D converters: Novel schemes and comparisons, IEEE Trans. Signal Process. 55 (5) (May 2007) 1769–1779.
[24] G. Jovanovic-Dolecek, S.K. Mitra, A new two-stage sharpened comb decimator, IEEE Trans. Circuits Syst. I 52 (7) (July 2005) 1414–1420.
[25] M. Laddomada, M. Mondin, Decimation schemes for $\Sigma\Delta$ A/D converters based on Kaiser and Hamming sharpened filters, IEE Proc. Vis. Image Signal Process. 151 (4) (August 2004) 287–296.
[26] G. Jovanovic-Dolecek, S.K. Mitra, A new multistage comb-modified rotated sinc (RS) decimator with sharpened magnitude response, IEICE Trans. E 88-D (7) (July 2005) 1331–1339.
[27] G. Jovanovic-Dolecek, S.K. Mitra, On design of CIC decimation filter with improved response, in: Proc. International Symposium on Communications, Control & Signal Processing, Malta, March 2008, pp. 1072–1076.
[28] G. Jovanovic-Dolecek, S.K. Mitra, Simple method for compensation of CIC decimation filter, Electron. Lett. 44 (9) (September 2008) 1162–1163.
[29] G.J. Dolecek, J.D. Carmona, A new cascaded modified CIC-cosine decimation filter, in: IEEE Conference ISCAS 2005, Kobe, Japan, May 2005, pp. 3733–3736.
[30] Y.C. Lim, R. Yang, On the synthesis of very sharp decimators and interpolators using the frequency-response masking technique, IEEE Trans. Signal Process. 53 (4) (April 2005) 1387–1397.
[31] J.O. Coleman, Chebyhev stopbands for CIC decimation filters and CIC-implemented array tapers in 1D and 2D, IEEE Trans. Circuits Syst. I. Regul. Pap. 59 (12) (December 2012) 2956–2968.

Gordana Jovanovic Dolecek received a BS degree from the Department of Electrical Engineering, University of Sarajevo, an MSc degree from University of Belgrade, and a PhD degree from the Faculty of Electrical Engineering, University of Sarajevo.

She was a full professor at the Faculty of Electrical Engineering, University of Sarajevo until 1993, and 1993–1995 she was with the Institute Mihailo Pupin, Belgrade.

In 1995 she joined Institute INAOE, Department for Electronics, Puebla, Mexico, where she works as a full professor.

During 2001–2002 and 2006 she was with Department of Electrical & Computer Engineering, University of California, Santa Barbara, and during 2008–2009 she was with San Diego State University, as visiting scholar. She was invited to hold lectures and short courses a number of times across the world. In 2012 she received Puebla State Award for science and technology.

She is reviewer for 15 SCI journals and many indexed international conferences, and she was a member of program committee for several international conferences. She was a guest editor of the journal ETRI Signal Processing, Special Issue on Advanced Techniques on Multirate Signal Processing for Digital Information Processing.

She is the author/co-author of four books, editor of one book, and author of 19 book chapters and more than 300 journal and conference papers.

Her research interests include digital signal processing and digital communications. She is a Senior member of IEEE, the member of Mexican Academy of Sciences, and the member of National Researcher System (SNI) Mexico.

Massimiliano Laddomada, Associate Professor of Electrical Engineering at Texas A&M University-Texarkana, received a PhD in Communications and Electronics Engineering from Politecnico di Torino in 2003. He is also an adjunct professor at California State University, Los Angeles since 2006. Prior to joining the Texas A&M University-Texarkana faculty on 2008, he worked as a visiting assistant professor at Polytechnic University of Turin (Italy) in 2003–2008, and as a senior engineer at Technoconcepts, Inc., Los Angeles in 2000–2001.

His main areas of research are digital signal processing and wireless communications, especially modulation and coding, including turbo codes and, more recently, molecular communications. From 2010 to 2012, he served as associate editor of IEEE Transactions on Circuits and Systems-I: Regular Papers. Currently he is an editor of IEEE Communications Surveys and Tutorials.